



ELSEVIER

Contents lists available at [SciVerse ScienceDirect](http://www.sciencedirect.com)

Journal of Luminescence

journal homepage: www.elsevier.com/locate/jluminLuminescence properties of Er^{3+} and Tm^{3+} doped BaY_2F_8 Ana C.S. de Mello^{a,*}, Adriano B. Andrade^a, Gerson H.G. Nakamura^b, Sonia L. Baldochi^b, Mário E.G. Valerio^a^a Physics Department, Federal University of Sergipe, 49, 100-000 São Cristóvão, SE, Brazil^b IPEN-CNEN/SP, CP 11049, 05422-970, São Paulo, SP, Brazil

ARTICLE INFO

Article history:

Received 17 March 2012

Received in revised form

15 October 2012

Accepted 4 December 2012

Available online 21 December 2012

Keywords:

 BaY_2F_8 Er^{3+} and Tm^{3+} doping

Scintillator

TL emission

Radiation damage

ABSTRACT

This paper reports the characterization of BaY_2F_8 doped with different concentrations of Er^{3+} and Tm^{3+} ions and their potential use as scintillators in radiation detection. Two types of samples were studied, polycrystalline samples, obtained via solid state reaction, and single crystals obtained via the zone melting method under a HF flow. The radioluminescence when excited with X-ray, showed emission peaks characteristics of the 4f–4f transitions of rare earths. Thermoluminescence measurements were done to study the traps that can inhibit the scintillating process. The radiation damage was evaluated and it was showed that the formation of the absorption bands can be connected to color centers generated by radiation in the matrix. Measurements of Dispersive X-ray Absorption Spectroscopy revealed that there is no change in the absorption edge of the dopant during irradiation indicating that the color centers are not connected to changes in the valence of the dopants but are direct connected to the defects due to the BaYF_2 matrix.

© 2012 Elsevier B.V. All rights reserved.

1. Introduction

In recent years the doped Barium Yttrium Fluoride (BaY_2F_8 – BaYF) gained attention because of possible applications as scintillator [1,2] and laser host [3,4]. Good candidates for high light yield are crystalline hosts that contains heavy metal ions combined with sites available for luminescent ions like the trivalent and some of the divalent rare earths (RE). In this particular sense BaYF is a very promising material that contains Ba^{2+} , a heavy metal with high electronic density, and Y^{3+} as site available for RE^{3+} doping. Other fluorides systems are reported in the literature and have gained considerable attention due to the properties of laser and “up conversion”. The LiYF henceforth referred to the LYF is particularly useful as a device material because rare earth ions can substitute Y^{3+} sites without the necessity for the charge compensating defect [5].

In the present work we have studied the luminescence properties of Er and Tm doped BaYF for application in scintillation devices and in radiation detection. Scintillators have a wide variety of applications in medicine and high energy physics [6].

The crystal structure of BaYF is monoclinic, and the trivalent rare-earth dopant ions are expected to occupy the Y^{3+} site [7]. The Y^{3+} site is coordinated with 8F^- ions having a C_2 point

symmetry [1]. Rare earth doped BaYF may be devised as scintillators [8] due to their high light output and also the useful wavelength emission that can be tuned by choosing the right rare earth dopant that matches the light detection device [2]. The objective of this paper is to understand the dependency between the scintillator properties as a function of doping concentration and understand the radiation damage generated in the samples after irradiation.

In the present work Er - and Tm - doped BaYF samples were prepared and studied via XRD powder diffraction, radioluminescence (RL) and thermoluminescence (TL). Radiation damage studied via optical absorption techniques can reveal the formation of the color centers generated by radiation in the matrix. The most probable defects in fluorides are F-type centers (F , F^- or F_A centers) and modified V_k centers [8]. Measurements of Dispersive X-ray Absorption Spectroscopy (DXAS) was done simultaneously with RL measurements to study the relation between the darkening of the sample due to the color centers and the possible relationship with the Er and Tm valence changes during irradiation.

2. Methodology

Polycrystalline samples of RE-doped BaYF were prepared in a platinum reactor from stoichiometric mixture of BaF_2 and YF_3 . ErF_3 is added in concentrations from 0.5, 1, 2, and 3 mol% and TmF_3 in concentrations of 1, 2 and 3 mol%. The starting materials were melted at 960°C [9] under a HF flow in Pt crucibles. The

* Correspondence to: Departamento de Física, Universidade Federal de Sergipe, 49100-000 São Cristóvão, SE, Brazil. Tel.: +55 79 21056636; fax: +55 79 21056807.
E-mail address: acarol_mello@yahoo.com.br (A.C.S. de Mello).

single crystals were prepared from the synthesized powders by the floating zone melting method, under HF atmosphere. Powder samples were prepared by grinding the obtained materials in an agate mortar and only the grains from 38 μm to 63 μm diameters were used.

The structural analyses of the polycrystalline and single crystals powdered samples were made by XRD measurements, performed at room temperature in a Rigaku DMAX Ultima+2000/PC diffractometer. The powder XRD patterns were taken in the 2θ range from 13 to 80° in step scan mode with steps of 0.02°, using $\text{CuK}\alpha$ radiation.

RL spectra were recorded exciting the samples with $\text{CuK}\alpha$ X-rays (40 KV/40 mA) at room temperature. The spectra were collected using an optical fiber conducting the light to an Ocean Optics HR2000 spectrometer. The scintillation efficient or light output for each sample can be obtained from the area under the RL spectrum.

The TL measurements were done from room temperature up to 400 °C following a linear heating program with a heating rate of 5 °C/s, in a homemade TL reader. The samples were irradiated with X-rays with dose of 0.0924 Gy.

The optical absorption was obtained via diffuse reflectance using a polychromatic light source (Mikropack DH-2000 UV-vis-NIR) and an optical fibers conducting the reflected light to Ocean Optics HR2000 spectrometer. All spectral measurements were corrected to the spectral response of the detecting apparatus.

Dispersive X-ray Absorption Spectroscopy (DXAS) measurements were done at the Brazilian Synchrotron Light Laboratory (LNLS) in the DXAS beamline (proposals 6754, 6707 and 7311). Polychromatic X-ray beam is tuned around the energy of the L_3 absorption edge of Er and Tm ions in a way that a full EXAFS spectrum is recorded in every 100 ms, using a CCD X-ray detector. The spectra were recorded as a function of the irradiation time in order to check if there is any change in the absorption edge of the dopant. At the same time, the RL was recorded so any changes in the emission spectra can be followed while the sample is irradiated.

3. Results and discussions

Fig. 1 presents the XRD powder patterns of polycrystalline samples and the single crystals with different concentrations of Er^{3+} and Tm^{3+} compared with the standard pattern [10]. It can be seen that only the expected BaY_2F_8 phase contributes to the

diffraction pattern. This indicates that the dopants were dissolved in the BaYF crystalline matrix.

Radioluminescence (RL) measurements were performed in order to determine the intensity and wavelength distribution of light output. Fig. 2 and Fig. 3 displayed the RL spectra of the Er^{3+} and Tm^{3+} doped BaYF powder, respectively, under irradiation with X-rays. The RL measurements of the doped BaYF showed emission peaks in energies that are characteristics of the 4f–4f transitions of the trivalent rare earth ions. Er^{3+} doped BaYF samples exhibited RL signals between 390 and 690 nm with maximum emissions at 542 nm due to the $^4\text{S}_{3/2} \rightarrow ^4\text{I}_{15/2}$ transition, corresponding to the green region of the visible spectrum. The single crystal samples with 2% Er^{3+} doped BaYF showed the highest RL intensity and the polycrystalline samples with 0.5% Er^{3+} showed the lowest intensity. The radioluminescence spectrum of Tm- doped BaYF with different concentration shows 4f–4f emission lines between 250 and 890 nm, with maximum emissions at 456 nm due to the $^3\text{P}_0 \rightarrow ^3\text{F}_4$ transition, corresponding to the blue region of the visible spectrum.

The total light yield of each scintillator can be obtained from the integration of its RL spectrum. Table 1 presents the scintillation efficient for each sample normalized to the intensity of the 2% Er doped single crystal samples that exhibited the highest intensity

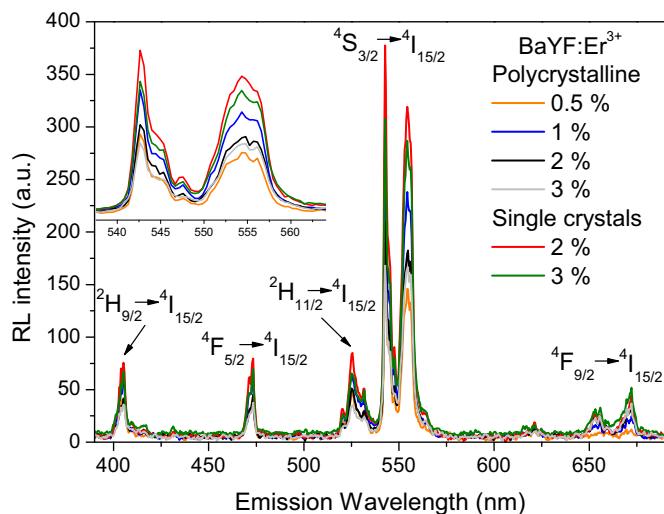


Fig. 2. RL spectra of the $\text{BaYF}:\text{Er}^{3+}$ single crystals and polycrystalline with different concentrations irradiated with X-rays. The inset shows the expanded region of the RL spectra around the main peak at 543 nm.

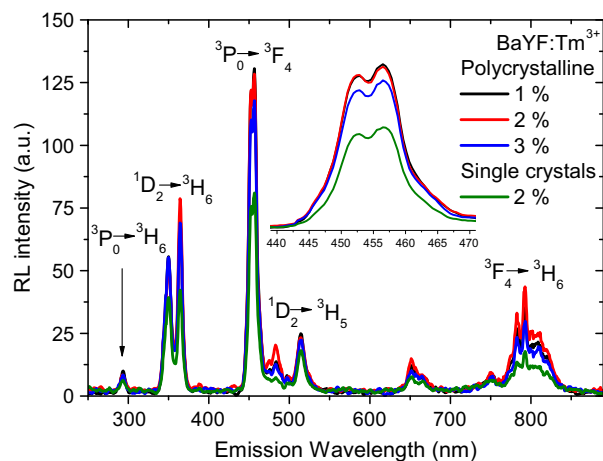


Fig. 3. RL spectra of the $\text{BaYF}:\text{Tm}^{3+}$ samples with different concentrations irradiated with X-rays.

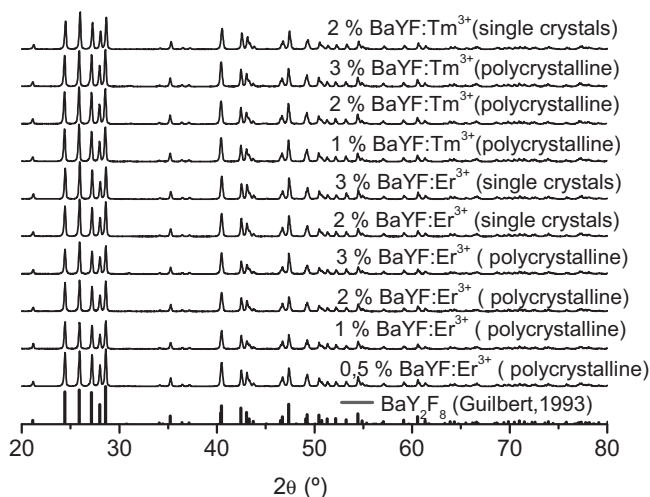


Fig. 1. XRD powder pattern of the polycrystalline samples and single crystals of $\text{BYF}:\text{Er}^{3+}$ and $\text{BYF}:\text{Tm}^{3+}$. The standard BaY_2F_8 pattern (Guilbert, 1993) is shown in the bottom of figure for comparison.

Table 1
Scintillation efficient of the BaYF:Er³⁺ of the Er- and Tm- doped BaYF samples.

Scintillation efficient	Er ³⁺	Tm ³⁺
0.5% Polycrystalline	43%	
1% Polycrystalline	84%	95%
2% Polycrystalline	63%	83%
3% Polycrystalline	59%	51%
2% Single crystal	100%	84%
3% Single crystal	90%	

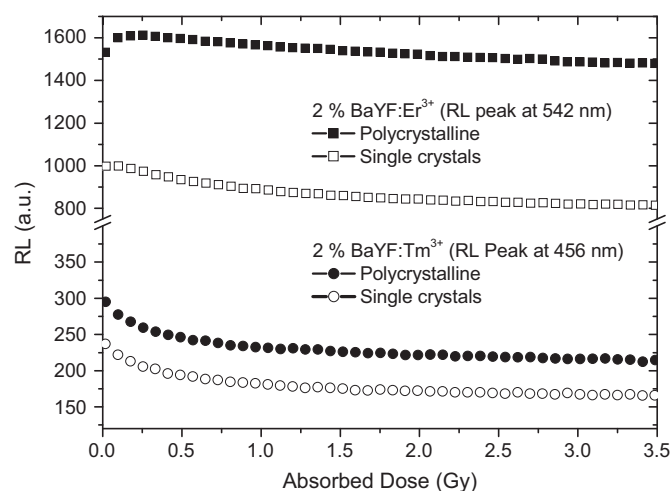


Fig. 4. RL intensity of peak in 542 and 456 nm of the BaYF:Er³⁺ and BaYF:Tm³⁺ as function with absorbed dose of the X-rays.

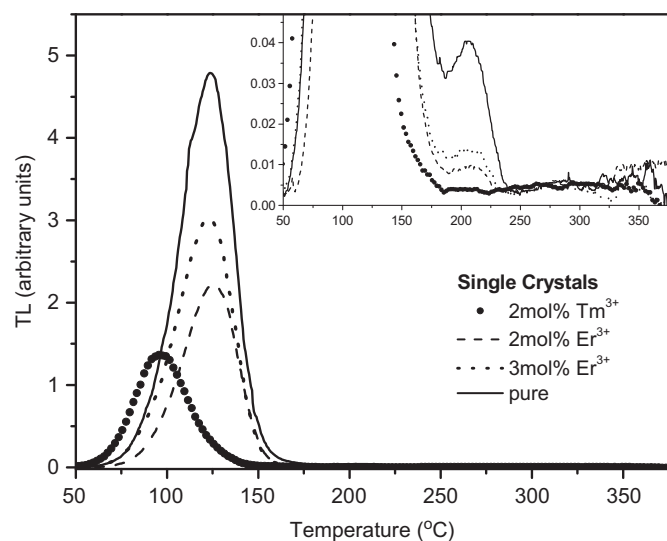


Fig. 5. Thermoluminescence of pure and Tm and Er doped BaYF single crystal, irradiated with a dose of 0.0924 Gy of X-rays.

among all samples. In the second column of Table 1 it can be seen that Er doped BaYF single crystals showed an increase in efficiency as compared to the polycrystalline samples, however the 1% sample stands out with the best efficiency of the polycrystalline samples. In column 3 it can be observed that, for Tm³⁺ doped BaYF samples, the RL efficiency is not proportional to the doping concentration. The decrease in scintillation efficiency for higher concentrations may be caused by aggregation of impurities which could lead to suppression of fluorescence. This hypothesis will be tested in future studies.

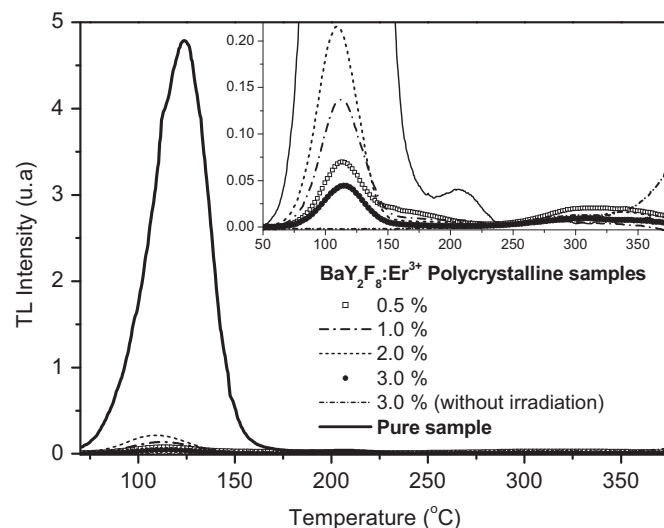


Fig. 6. Thermoluminescence of pure and Er doped BaYF polycrystalline, irradiated with a dose of 0.0924 Gy of X-rays.

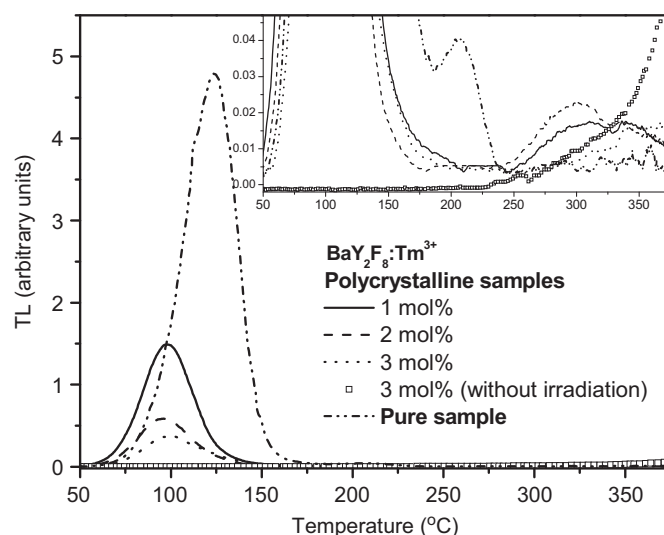


Fig. 7. Thermoluminescence of pure and Tm doped BaYF polycrystalline, irradiated with a dose of 0.0924 Gy of X-rays.

All the samples presented radiation damage and this is related to the change of scintillation efficiency due to defect creation by the radiation dose [11]. Fig. 4 shows RL intensity of main peak at 542 nm, for both 2% Er doped BaYF single crystals and polycrystalline samples, and the main peak at 456 nm, for the 2% Tm doped BaYF single crystals and for the polycrystalline sample, as a function with the absorbed dose. The figure indicates the buildup of radiation damage. The BaYF:Er³⁺ single crystal samples showed an increase for initial doses followed by a decrease of the RL intensity. At about 3.0 Gy the RL intensity seems to stabilize at slightly lower level than the initial one. The polycrystalline sample showed, apart from a very small increase of the RL intensity for lower doses, a steady decrease up to ~3.0 Gy. The BaYF:Tm samples, on the other hand, showed a fast decrease for doses up to ~1.0 Gy following by a steady state, almost linear, decrease of the RL intensity as a function of the absorbed dose.

The Figs. 5–7 show the thermoluminescence glow curves of the pure and doped samples. All glow curves displayed one very intense peak at low temperature in the range from 50 to 370 °C. For the undoped single crystals and all Er-doped samples, this TL

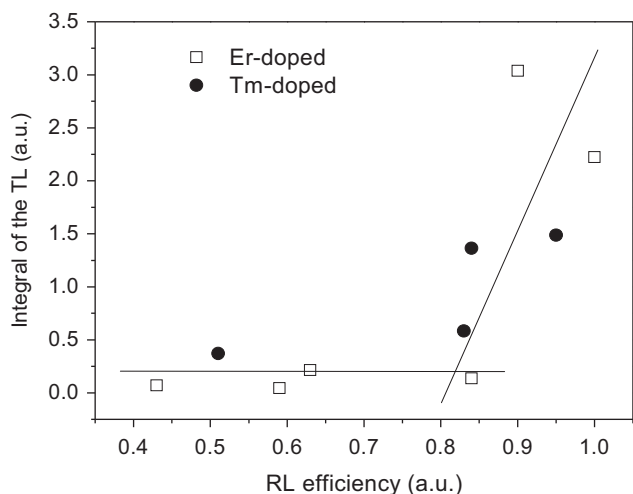


Fig. 8. RL intensity vs. TL intensity for all Er and Tm doped samples. The lines are just guides for the eyes.

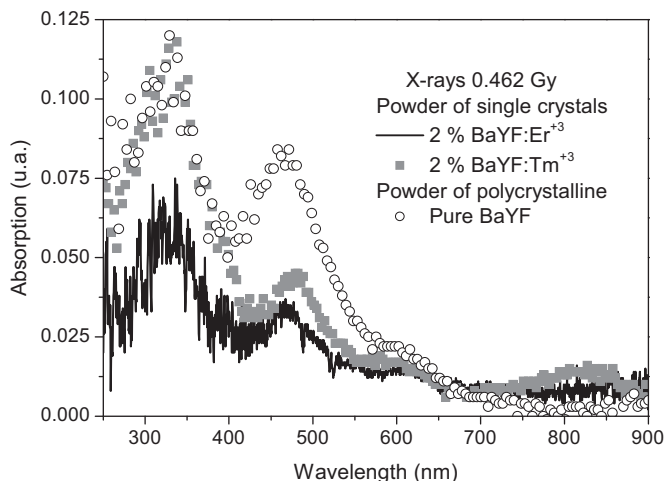


Fig. 9. Optical absorbance spectra of pure and Er and Tm doped BaYF samples irradiated with 0.462 Gy of X-rays. The non-irradiated samples were used as the reference absorption.

peak is located at 123 °C. While for all Tm³⁺ doped BaYF samples there was a shift of this peak to 100 °C. Besides this peak, there are other less intense peaks at 205, 300 and 340 °C. The 205 °C peak is noticeable mainly in the single crystals while the other high temperature peaks are visible in the polycrystalline ones.

The highest TL yield, corresponding to the total area under the TL curve, is obtained for the pure samples. Among the doped ones, single crystal samples of BaYF doped with 3% of Er³⁺ presented higher TL intensity. But, at the same time, this sample presented one of the highest RL efficiency (see Table 1). Also, the TL peak position did not change when different dopant concentration are considered, indicating that the trap depths are not influenced by the concentration of the dopant. On the other hand, there is a strong influence on the dopant concentration on the TL intensity.

The correlation between TL and RL can be better seen in Fig. 8 where the density of trapping associated to the overall TL emission (that is proportional to the area under the TL glow curves), were plotted as a function of the normalized RL efficiency (area under the RL spectra) for all doped samples. The figure shows that up to 0.8 in RL efficiency, there is almost no dependence on the TL but above that the RL quickly grew as the TL intensity increased. This is quite unexpected result since usual models of TL and RL point out that there should be a competition between both processes and the

highest TL intensity is normally found for materials not showing good scintillation efficiency. The present result indicates that the usual model does not always apply and in the specific case of doped BaY₂F₈ new models should be devised to interpret these findings.

All Er and Tm doped BaYF samples became dark after irradiation due to the buildup of radiation damages. The coloration of the sample was evaluated by optical absorption obtained from the reflectance spectra of the irradiated powder samples. The results are shown in Fig. 9 for pure and the doped samples irradiated with 0.462 Gy of X-rays. Three main absorptions bands are observed in all samples with maximum approximately at 327, 462 and 612 nm. Powder samples from single crystal doped with 2% of Tm³⁺ showed an extra band at about 827 nm. All spectra are very noisy but it is also possible to notice the absence of the sharp absorption lines due to the rare earth dopants. This can be explained if we take into account that the amount of dopant is small compared to the very strong bands due to the radiation damage. Another interesting result shown in this figure is that the position of the three main absorption bands due to the radiation induced color centers are independent of doping, but the relative intensity of them seems to show a slight variation depending on the dopant. This is a strong indication that the defects centers generated by irradiation are mainly linked to the BaYF matrix. The most probable defects in fluorides are F centers, F_A centers and modified V_k centers that are known to produce absorption bands in the 300–330 nm, 240–380 nm, 450–600 nm regions [12,13].

Another possible source of changes in coloration due to irradiation would be change in the valence of the dopants and that can be checked measuring the X-ray absorption near edge (XANES) while the sample is irradiated. This is shown in Fig. 8 for Er doped polycrystalline samples. In the same figure, a XANES spectra of the Er ions in the standard compound Er₂O₃ measured in the same setup conditions is shown for comparison. In Er₂O₃, Er ions are known to be only in the trivalent state. It can be seen that the absorption near edge of the Er doped BaYF samples is very close to the Er found in Er₂O₃ compounds during the time span of the experiment. This result is a strong indication that there is no change in the absorption edge during the whole period of irradiation. The three measurements taken 1 min, 20 min or 40 min after switching on the X-rays did not show any significant change. During the whole irradiation time XANES spectra were collected every 600 ms and no changes were observed. In Fig. 10 just 3 representative spectra were shown. The only difference is the signal to noise ratio that is worse in the Er doped BaYF due to the small amount of Er in the matrix as compared to the Er₂O₃ sample.

Similar result was observed for BaYF:Tm. The XANES measurements for the 2 mol% doped polycrystalline as compared to the absorption edges of the Tm ions in the standard compound TmF₃ is presented in Fig. 10.

Radioluminescence (RL) measurements were taken simultaneously with the XANES measurements and a full RL emission spectra was recorded every 300 ms. The results are shown in Fig. 11 for BaYF:Er³⁺ and BaYF:Tm³⁺ samples, respectively. One can see that there is no change in the positions of the RL peaks during irradiation, only a change in RL intensity due to radiation damage. The DXAS-XANES results combined to the simultaneous measurements of the RL indicates clearly that there is no direct participation of the Er and Tm ions in the creation of the radiation damage since no evidence of valence change or change in the emission spectra were found during irradiation.

4. Conclusions

This work demonstrated that BaYF doped Er and Tm is an interesting material for radiation detection and possible applications in scintillators. For the Tm³⁺ doped BaYF samples the light output efficiency is not proportional to the doping concentration and Er³⁺

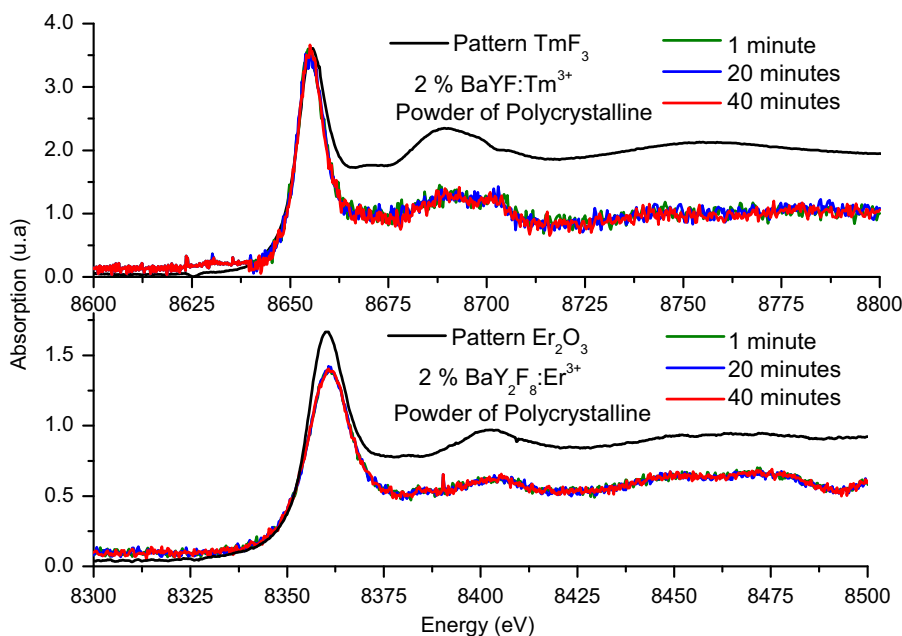


Fig. 10. Comparison of the XANES measurements close to the absorption edge of Tm^{3+} ions in BaYF sample, compared to the XANES of TmF_3 standard materials [upper plot]. Comparison of the XANES measurements near the absorption edge of Er^{3+} ions in BaYF sample, compared to the XANES of Er_2O_3 standard materials [bottom plot]. The measurements were done using the DXAS beamline at the LNLS.

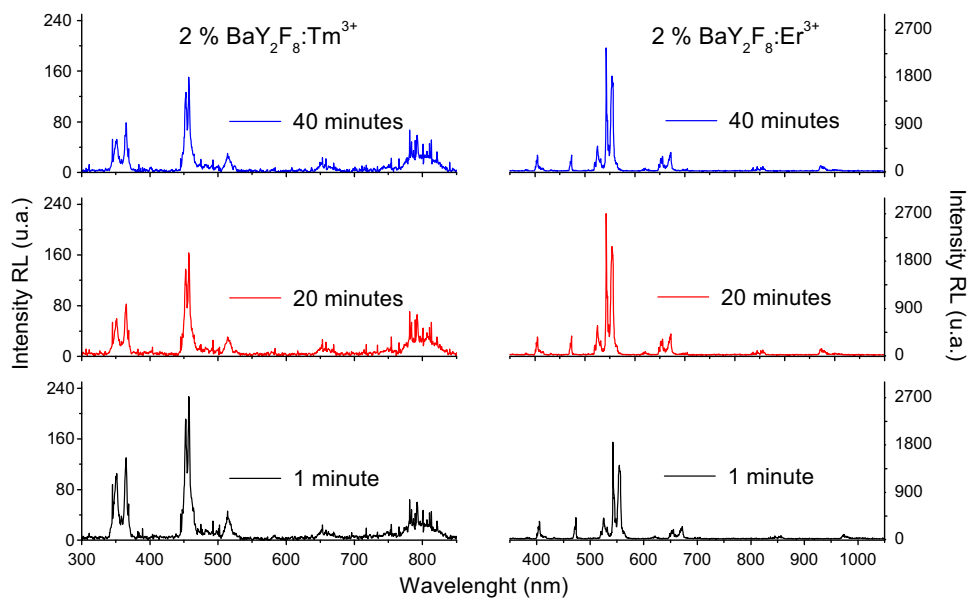


Fig. 11. RL spectra of the 2% $\text{BaY}_2\text{F}_8:\text{Er}^{3+}$ and $\text{BaY}_2\text{F}_8:\text{Tm}^{3+}$ polycrystalline samples irradiated with synchrotron light at three times made simultaneously with DXAS measurements.

doped presented best efficiency in the form of single crystals samples. The TL curves presented the same main peak for all the samples studied, including pure and doped samples, indicating that both Er and Tm doped samples have the same trap distribution mainly due to defects in the matrix. All samples presented radiation damage creating absorption bands that can be connected to color centers generated during radiation. This radiation damage influences the RL intensity. On the other hand, combination of Dispersive X-ray absorption measurements with simultaneous RL measurements, revealed that the Er and Tm dopants did not directly participate in the formation of the color centers induced by radiation, supporting the assumption that these color centers are connected to defects in the BaYF matrix.

Acknowledgments

The authors gratefully acknowledge the CNEN, CAPES, CNPq and FAPES for financial support. The authors also acknowledge the LNLS (Brazilian Synchrotron Light Laboratory) for the support and the use of the DXAS and XAFS beamlines (proposals XAFS 6743 and 7285, and DXAS 6754, 6707 and 7311)

References

- [1] J.C. van't Spijker, et al., *J. Lumin.* 85 (1999) 11.
- [2] M.E.G. Valerio, V.G. Ribeiro, A.C.S. Mello, M.A.C. Santos, S.L. Baldochi, V.L. Mazzocchi, C.B.R. Parente, R.A. Jackson, J.B. Amaral, *Opt. Mater.* 30 (2007) 184.

- [3] F. Cornacchia, D. Parisi, C. Bernardini, A. Toncelli, M. Tonelli, *Opt. Express* 12 (2004) 1982.
- [4] S. Bigotta, D. Parisi, L. Bonelli, A. Toncelli, A. Di Lieto, M. Tonelli, *Opt. Mater.* 28 (2006) 1321.
- [5] G.M. Renfro, J.C. Windscheif, W.A. Sibley, *J. Lumin.* 22 (1980) 51.
- [6] G. Blasse, *Chem. Mater.* 6 (1994) 1465.
- [7] J.B. Amaral, M.A.C. Santos, M.E.G. Valerio, R.A. Jackson., *Appl. Phys.* 81 (2005) 841.
- [8] A.C.S. de Mello, A.B. Andrade, G.H.G. Nakamura, S.L. Baldochi, M.E.G. Valerio, *Opt. Mater.* 32 (2010) 1337.
- [9] G.H.G. Nakamura, S.L. Baldochi, V.L. Mazzocchi, C.B.R. Parente, M.E.G. Valerio, D. Klimm, *J. Therm. Anal. Calorim.* 95 (1) (2009) 43.
- [10] L.H. Guilbert, J.Y. Gesland, A. Bulou, R. Retoux., *Mater. Res. Bull.* 28 (1993) 923.
- [11] C. Greskovich, S. Duclos., *Annu. Rev. Mater. Sci.* 27 (1997) 69.
- [12] M.K. Stawomir, B. Amina, B. Georges., *Opt. Mater.* 28 (2006) 123.
- [13] G.M. Marolo, G. Baldachini, V.S. Kalinov, E.R.M. Monterealli, *Phys. Status Solidi (c)* 2 (2005) 367.